Two Types of Distribution Patterns of Bigeminy and Trigeminy in Long-Term ECG: a Model-Based Interpretation

N Ikeda[1], K Takayanagi[2], A Takeuchi[1], N Mamorita[1], H Miyahara[3]

[1]Department of Medical Informatics, Kitasato University, Sagamihara, Japan
[2]Department of Cardiology, Dokkyo University, Koshigaya, Japan
[3]Department of Rehabilitation, Toyohashi SOZO University, Toyohashi, Japan

Abstract

Two types of distribution patterns of bigeminy and trigeminy are found in analysis of long-term ECG. To investigate the mechanism underlying this finding, a simplified equation of a modulated parasystole model was used and symbolic solutions for cyclic VPC patterns were obtained. The map of these solutions in a model parameter plane showed two different solutions for bigeminy, four kinds of trigeminy, two kinds of quadrigeminy, combinations of these patterns, and apparently normal ECG. These results are used to explain the features of the distribution patterns.

1. Introduction

1.1. Background and purpose

The rate of appearance of ventricular premature contraction (VPC) depends on heart rate (HR) in analyses of a Holter ECG and in exercise stress tests. Different patterns of HR-dependency in VPC have been reported: an increase in VPC frequency as HR increases, a decrease in VPC frequency, non-monotonous changes, and disappearance of VPC at a specific HR. Nakata and Takayanagi reported two types of distribution patterns of bigeminy and trigeminy in plots of VPC frequency in a Holter ECG using the coupling interval between each VPC and the next normal sinus beat (XN) as the abscissa, where "X" designates a VPC and "N" is a normal sinus beat [1-3]. On this histogram, a trigeminy-bigeminy order of appearance (with increasing XN) was defined as the standard type and a bigeminy-trigeminy order as the reverse type. The purpose of the current study is to provide an interpretation of this phenomenon using a mathematical model of parasystole.

1.2. Two types of distribution patterns of bigeminy and trigeminy

ECG recordings are shown in Figure 1. In the X-N sequence, a pattern XNX is defined as bigeminy and XNNX as trigeminy. Figure 1 shows two cases of Holter ECGs. In Figure 1A, the XN interval for bigeminy is larger than that for trigeminy, and in Figure 1B, the XN interval for trigeminy is larger than that for bigeminy. Histograms of bigeminy (blue) and trigeminy (yellow) over long ECG recordings are shown in Figures 2 and 3.
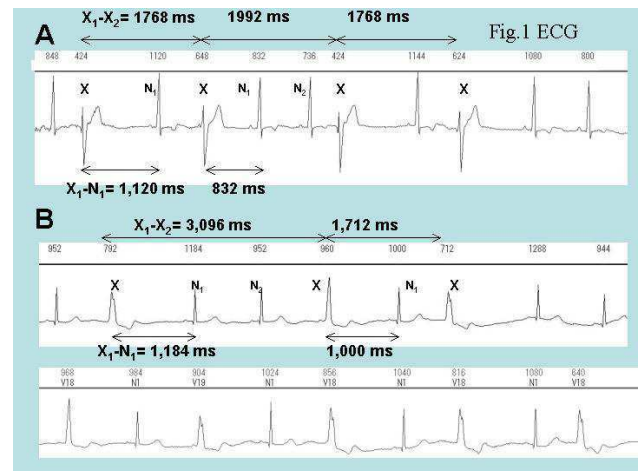

Figure 1. Two types of bigeminy-trigeminy patterns. A: standard type in which the bigeminy distribution is centered at a larger XN, and B: reverse type in which the bigeminy distribution occurs at a smaller XN.
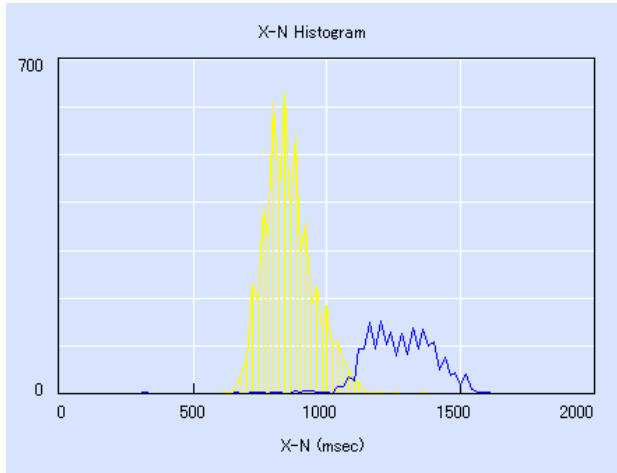
Figure 2. Histogram of bigeminy (blue) and trigeminy (yellow) for XN values (standard type).
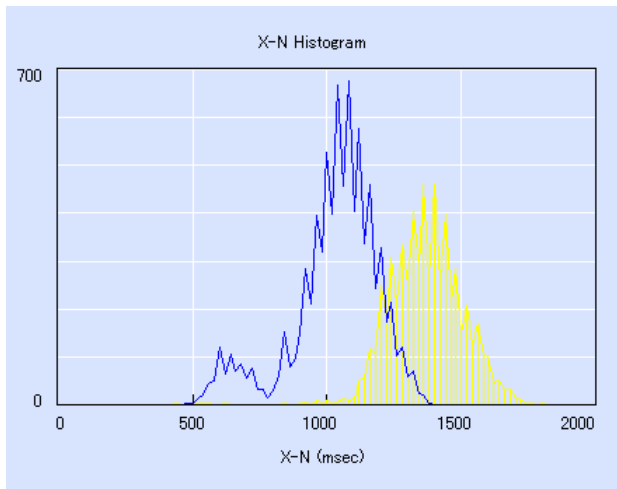

Figure 3. Histogram of bigeminy (blue) and trigeminy (yellow) for XN values (reverse type).

Two types of patterns were distinguished: the standard type (Figure 2) in which the bigeminy distribution is centered at a larger XN, and the reverse type (Figure 3) in which the bigeminy distribution occurs at a smaller XN.

2. Methods

We assumed a *modulated parasystole model* and formulated the model as a system of difference equations in a phase of the sinus pacemaker's stimulus on an ectopic pacemaker. Assuming that the variable t_n is the n-th phase of the ventricular excitation induced by the sinus pacemaker in the oscillation of the ectopic pacemaker, the following equations are obtained between the successive phases, t_n and t_{n+1} [4, 5].

$$t_{n+1} = \begin{cases} t_n + Ts - PRC\,(t_n) & (0 \le t_n < Te) & (1N) \\ t_n - Te + Ts & (Te \le t_n < Te + (1-\gamma)Ts\,) & (1X) \\ t_n - Te & (Te + (1-\gamma)Ts \le t_n < Te + Ts) & (1\,.) \end{cases}$$

where Ts is the intrinsic period of the sinus pacemaker, Te is the intrinsic period of the ectopic pacemaker, and γTs is the refractory period due to the sinus R wave. The function $PRC\,(t)$ represents the phase response curve (PRC) of an ectopic pacemaker.

Approximating the PRC function by

$$PRC(t) = \begin{cases} a\,t & (t \le wTe) \\ b(t - Te) & (t > wTe), \end{cases}$$

where w is a break point of the PRC, equation (1N) becomes

$$t_{n+1} = \begin{cases} (1 - a)\,t_n + Ts & (0 \le t_n < wTe) & (1a) \\ (1 - b)\,t_n + bTe + Ts & (wTe \le t_n < Te) & (1b) \end{cases}$$

and equation (1) becomes

$$t_{n+1} = \begin{cases} (1 - a)\,t_n + Ts & (0 \le t_n < wTe) & (1a) \\ (1 - b)\,t_n + bTe + Ts & (wTe \le t_n < Te) & (1b) \\ t_n - Te + Ts & (Te \le t_n < Te + (1-\gamma)Ts\,) & (1X) \\ t_n - Te & (Te + (1-\gamma)Ts \le t_n < Te + Ts) & (1\,.) \end{cases}$$

Equations (1a) and (1b) correspond to a normal beat, equation (1X), an ectopic beat, and equation (1 .), a silent ectopic beat that is concealed under the refractory period of the ventricle. We define a cyclic solution with period n of (1) to be a sequence $\{t_0, t_1, \ldots, t_n\}$ with $t_n = t_0$, and the solution is represented as $\{bX\}$, $\{abX\}$, $\{b.aX\}$, etc., using symbols that correspond to the branches of equations (1a), (1b), (1X) and (1 .).

A symbolic formula processor (MathCad8, MathWorks Inc.) was used to obtain stable solutions of ECG patterns.

3. Results

3.1. Regions of stable solutions

Theoretically, we obtained stable solutions for bigeminy ({bX} and {aX}), trigeminy ({bbX}, {abX}, {b.bX} and {b.aX}), quadrigeminy, and apparently normal ECG. Patterns of bigeminy and trigeminy and the corresponding regions with respect to Ts were obtained as follows:

Bigeminy {bX}:
$$\max[(1- b+w\,b)Te/2, (1-b)Te/(2-b)]$$
$$\leq Ts < (1-b)Te/(2-2b+\gamma b) \qquad (2)$$
Bigeminy {aX}:
$$Te/(2-a) \leq Ts <$$
$$\min[(1+ wa)Te/2, Te/(2-2a+\gamma a)] \qquad (3)$$
Trigeminy {bbX}:
$$\max[(1- b+w\,b)Te/2, (1-b)Te/(2-b)]$$
$$\leq Ts < \min[(1+ wa)Te/2,$$
$$Te/(2-2a+\gamma a)]\,(1-b)Te/(2-2b+\gamma b) \qquad (4)$$
Trigeminy {abX}:
$$\max[(1-b)Te/(3-b), (1-a-b+ab+w(a+b-ab))Te/$$
$$(3-2b), (1- b)Te/(3-a-2b+ab)] \leq Ts$$
$$< \min[(1-b+w(a+b-ab))Te/(3-b), Te/(3-2a),$$
$$(1-b)Te/(3-2a+2ab+\gamma(a+b-ab))] \qquad (5)$$
Trigeminy {b.bX}:
$$\max[(2-b)(1- b+w\,b)Te/(3-b), (1-b)(2-b)Te/$$
$$(3-4b+b^2+\gamma b(2-b)), (2-b)(1-b+wb)Te/(3-2b),$$
$$(1-b)(2-b)Te/(3-4b+b^2+\gamma b(2-b))]$$
$$\leq Ts < \min[(2-b)Te/(3-b),$$
$$(1-b)(2-b)Te/(3-5b+2b^2+\gamma b(2-b))] \qquad (6)$$
Trigeminy {b.aX}:
$$\max[(2-b)(1- b+w\,b)Te/(3-b), (1-b)Te/$$
$$(3-2b-(1-\gamma)(a+b-ab)), (1-b)Te/(3-2b),$$
$$(2-a-b+ab)Te/(3-2a-b+ab)] \leq Ts <$$
$$\min[2Te/(3-a), (2-2b+w(a-b+ab))Te/(3-2a),$$
$$(2-a-b+ab)Te/(3-a+(2-\gamma)(a+b-ab))] \qquad (7)$$

etc.

A map of these regions was drawn as two-dimensional areas in the Ts/Te - w plane (Figure 4). We also derived a linear relationship between XN and Ts as follows: for the solution {bC} to exist, $t_0 = XN$ satisfies $wTe \leq t_0 < Te$, $t_1 = (1-b)t_0+bTe+Ts$ obtained from equation (1b) satisfies $Te \leq t_1 < Te+(1-\gamma)Ts$, and $t_2 = t_1 - Te + Ts$ obtained from equation (1X) must satisfy $t_2 = t_0$. Solving these equations gives region (2) for Ts, and the relationship between XN ($= t_0$) and Ts as follows:

$$XN = (2Ts - (1-b)Te)/b \qquad (6).$$

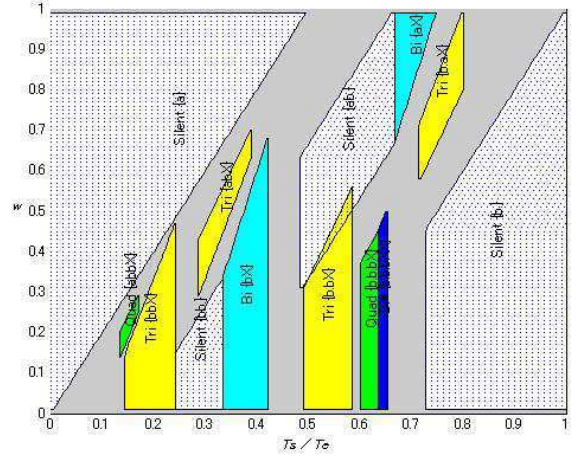Similar relationships can be obtained for other solutions.

Figure 4. Regions of stable solutions in the Ts/Te-w plane, including two of bigeminy (cyan), four of trigeminy (yellow), and two of quadrigeminy (green). Between these regions, combinations of the patterns (gray) and silent patterns (dots) are shown. Parameters: $a = b = 0.5$ and $\gamma = 0.375$.
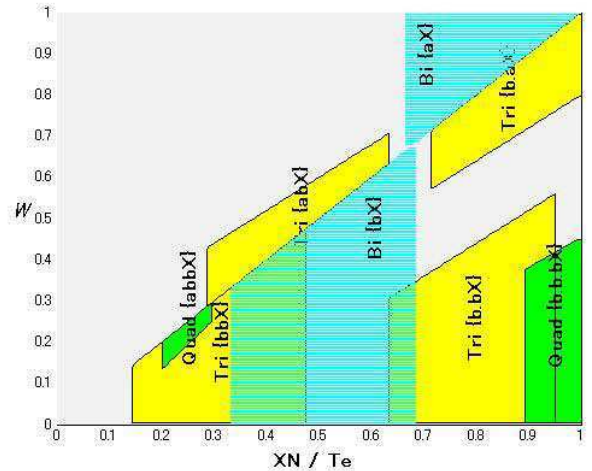

Figure 5. Regions of bigeminy (cyan), trigeminy (yellow) and quadrigeminy (green) in the XN/Te-w plane.

Thus we have a solution map in the *XN/Te-w* plane (Figure 5). Clinically observed VPC distributions were explained from this map: when *XN/Te* is small, bigeminy {bX} is preceded by trigeminy {bbX} (for small w) or by {abX} (for large *w*) as *XN* increases, the standard type pattern (Figure 2); and when *XN/Te* is large, bigeminy {bX} is followed by trigeminy {b.bX}, the reverse type pattern (Figure 3).

3.2. Computer simulation

The results shown in Figures 4 and 5 indicate regions of steady-state solutions of equation (1), i.e., under conditions in which the model parameters were held constant. Clinically observed distributions (Figures 2 and 3) arose from conditions of long-term variation of biological parameters. To simulate these results, computer simulations were performed using equation (1) with random fluctuations of the parameters *Ts* and *w*. The results are shown in Figure 6 as a histogram of frequency of bigeminy and trigeminy.
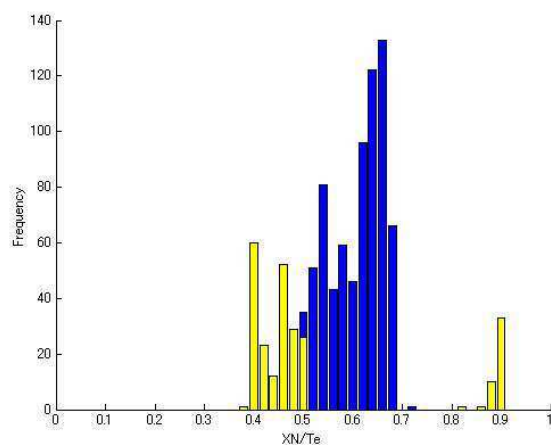

Figure 6. Histogram of bigeminy (blue) and trigeminy (yellow) for XN values obtained from the computer simulation.

The values of *Ts* and *w* were changed randomly at a certain period of time according to a normal distribution. The two types of distributions (standard and reverse) appear in the same graph because of the wide variation in parameter values.

4. Discussion and conclusions

We have shown that the two clinically observed types of distribution patterns of bigeminy and trigeminy and their related properties can be explained by the modulated parasystole model, although other mechanisms such as reentry and delayed afterdepolarization cannot be excluded.

Acknowledgements

References

[1] Nakata T: Study of the inter-ectopic intervals of ventricular premature contractions with a fixed coupling interval. Dokkyo J Med Sci 2002; 11, 168-177 (in Japanese).

[2] Takayanagi T, et al.: Distribution patterns of bigeminy and trigeminy discriminate two types of ventricular parasystole (in preparation).

[3] Takayanagi T, Kamishirado H, Iwasaki Y, Fujito T, Sakai Y, Inoue T, Hayashi T, Morooka S: Cyclic bursts of ventricular premature contractions of more than one minute intervals. *Jpn Heart J* 1999; 40:135-144.

[4] Ikeda N, Takeuchi A, Hamada A, Goto H, Mamorita N, Takayanagi K: Model of bi-directional modulated parasystole as a mechanism for cyclic bursts of ventricular premature contractions. Biol Cybern 2004; 91: 37-47.

[5] Ikeda N, Yoshizawa S, Sato T: Difference equation model of a ventricular parasystole as an interaction between cardiac pacemakers based on the phase response curve. *J Theor Biol 1983;* 103: 439-465.

Address for correspondence

Noriaki Ikeda
Department of Medical Informatics
Kitasato University School of Allied Health Sciences
Kitasato 1-15-1, Sagamihara, Kanagawa 228-8555, Japan
ikeda@kitasato-u.ac.jp